Acta Cryst. (1990). **B46**, 693–698

Bi Ordering in High-Temperature Structures of $BaBiO_{3-x}$

By Hiroshi Sakuma and Hiroo Hashizume

Research Laboratory of Engineering Materials, Tokyo Institute of Technology, Nagatsuta, Midori-ku, Yokohama 227, Japan

and Atsushi Yamanaka

Central Research Laboratory, Sumitomo Metal Mining Co. Ltd, Nakakokubun 3-18-5, Ichikawa 272, Japan

(*Received* 6 *April* 1990; *accepted* 13 *June* 1990)

Abstract

Rietveld refinements of neutron powder diffraction data have revealed that cubic $BaBiO_3$ at 900 K contains a breathing-mode displacement of O ions in a perovskite-like structure, indicating an ordered array of Bi^{3+} and Bi^{5+} ions as in the lower-temperature forms of the crystal. The structural features are preserved in phase I of oxygen-deficient $BaBiO_{3-x}$ at 1025 K, consistent with the semiconductor-like properties of the material. Cubic $BaBiO_{3-x}$ in a more-reduced phase II material at 1075 K is oxygen deficient and shows no apparent O shift. The observed semiconductor–metal-like transition at the I–II phase boundary does not contradict the 4+ valence state of the Bi cations in cubic $BaBiO_{3-x}$ of phase II. The refinements indicate oxygen-deficient tetragonal structures coexisting with more abundant cubic structures in phase I and II materials.

1. Introduction

The valence state and ordering of Bi cations in the perovskite-like oxide $BaBiO_{3-x}$ has been a matter of continued interest. The monoclinic crystal structure of $BaBiO_3$ at room temperature contains two distinct Bi sites characterized by average Bi—O distances of 2·28 and 2·12 Å. This has been taken to indicate an ordered arrangement of Bi^{3+} and Bi^{5+} cations at unequal BiO_6 octahedra (Cox & Sleight, 1976, 1979), although the results of infrared (de Hair & Blasse, 1973) and X-ray photoemission (Orchard & Thornton, 1977; Wertheim, Remeika & Buchanan, 1982) measurements, as well as those of electronic structure calculations (Mattheiss & Hamann, 1983), suggest marginal differences in the charge distributions at the two Bi ions. In fact, $BaBiO_3$ is the first example of an $A_2BB'O_6$-type perovskite in which the ordered B-site ions are the same element. The room-temperature monoclinic structure of $BaBiO_3$ transforms into a rhombohedral form at 405 K and then into a cubic form at 750–800 K (Cox & Sleight, 1976, 1979). Rietveld refinements of high-temperature neutron powder data indicate essentially unchanged Bi—O distances between 298 and 723 K, and therefore preserved Bi valence and ordering situations at the monoclinic–rhombohedral transition. Cox & Sleight (1979) describe the BiO_6 octahedra as rigid structural units which can vary in orientation with temperature, but not in shape and size even at the phase transition. The ordered Bi structure is apparently consistent with the semiconducting properties of the material, which have been confirmed up to 973 K (Cox & Sleight, 1979). It is thus very likely that cubic $BaBiO_3$ is also ordered. However, our previous study found no evidence of Bi ordering in neutron powder data collected at 900 K (Kusuhara, Yamanaka, Sakuma & Hashizume, 1989). The ordered cubic structure would be characterized by shifted O ions in a doubled perovskite cell, which we failed to detect in our diffraction data.

Meanwhile, the Rietveld profile-fitting program *RIETAN* (Izumi, Asano, Murata & Watanabe, 1987) has been modified for the analysis of neutron powder data collected on the HRP diffractometer at the KENS spallation-source facility. The new version uses a fitted profile for incident-beam monitor counts, and can thus better fit weak Bragg peaks sitting on a fluctuating background with low neutron counts. *RIETAN* defines the background by a five-order polynomial in time-of-flight, which is refined simultaneously with the lattice-constant, peak-shape and individual anisotropic thermal parameters.

In the present paper the new version of *RIETAN* is used to re-examine the high-temperature powder data collected from $BaBiO_{3-x}$ compounds by Kusuhara *et al.* (1989). Attention is focused on the O positions in cubic structures in materials with well-controlled oxygen deficiencies ($x = 0$–$0{\cdot}2$). Also reported are electrical resistivity measurements, which provide information on the valence state of Bi cations when combined with the structural results.

0108-7681/90/060693-06$03.00

2. Bi ordering in cubic $BaBiO_3$

The new *RIETAN* program was tested by refining the neutron data obtained from a ceramic $BaBiO_3$ sample at 900 K under a controlled O_2-gas partial presssure of 1 kPa. A least-squares refinement was initially carried out on a simple perovskite structure (space group $Pm\bar{3}m$) with a cell parameter a_0. We fixed the O-site occupancy parameter at 1. This resulted in a slightly better fit with $R_{wp} = 4{\cdot}68$, $R_p = 3{\cdot}53$, $R_e = 2{\cdot}85$, $R_I = 3{\cdot}89$ and $R_F = 5{\cdot}26\%$ as compared with Fig. 5 of Kusuhara *et al.* (1989). For definitions of the *R* factors, see Rietveld (1969) and Young & Wiles (1982).

The same intensity data were also examined for a doubled ($2a_0$) perovskite cell with space group $Fm\bar{3}m$. The variable O position parameter x(O) was given a small displacement from the ideal value of 0·25. In the course of refinement, some unexplained small peaks were found to be ascribable to Bragg reflections from mullite, which was used in the sample chamber. Probably, at the time of data collection, the primary neutron beam hit the edge of openings bored in the wall of a mullite tube placed around the sample. Refinements were then repeated on a two-component system consisting of orthorhombic silicon–mullite and cubic $BaBiO_3$. Starting structural parameters for mullite were taken from Saalfeld & Guse (1981), but only the cell parameters were refined. The Rietveld profile fit converged to the *R* factors $R_{wp} = 4{\cdot}22$, $R_p = 3{\cdot}21$, $R_e = 2{\cdot}85$, $R_I = 4{\cdot}19$ and $R_F = 6{\cdot}46\%$, with a refined O position of $x(\mathrm{O}) = 0{\cdot}2605\,(4)$ for $BaBiO_3$. Although these values are lower than those for the $Pm\bar{3}m$ model, one cannot jump to a conclusion in favor of the $Fm\bar{3}m$ model. In Fig. 1,* where the results of the three fits are compared on an expanded intensity scale, a set of $BaBiO_3$ reflections with *h*, *k* and *l* all odd are satisfactorily explained by the ordered doubled-cell model (*c* and *d*). These superlattice reflections are forbidden in the simple-cell model (Fig. 1*b*) and have no more than 3% of the intensity of the strongest peak. The finite observed intensities manifest doubling of the cell edges owing to the oxygen shift. The refined structure shows Bi—O bond lengths of 2·29 (9) and 2·09 (9) Å. These are very close to the values quoted above, confirming the presence of rigid BiO_6 octahedra. Unlike the previous X-ray analysis (Kusuhara *et al.*, 1989), the refined anisotropic thermal parameters for the Bi and O ions are not accompanied by large standard deviations. Also, the refined mullite cell parameters compare favorably with documented values. All these factors point to a successful structure refinement, and lead to the conviction that cubic $BaBiO_3$ is ordered with a 'breathing-mode' distortion resulting from an O-ion

---

* Data for the observed and calculated profiles for $BaBiO_{3-x}$ at 900, 1025 and 1075 K have been deposited with the British Library Document Supply Centre as Supplementary Publication No. SUP 53322 (191 pp.). Copies may be obtained through The Technical Editor, International Union of Crystallography, 5 Abbey Square, Chester CH1 2HU, England.

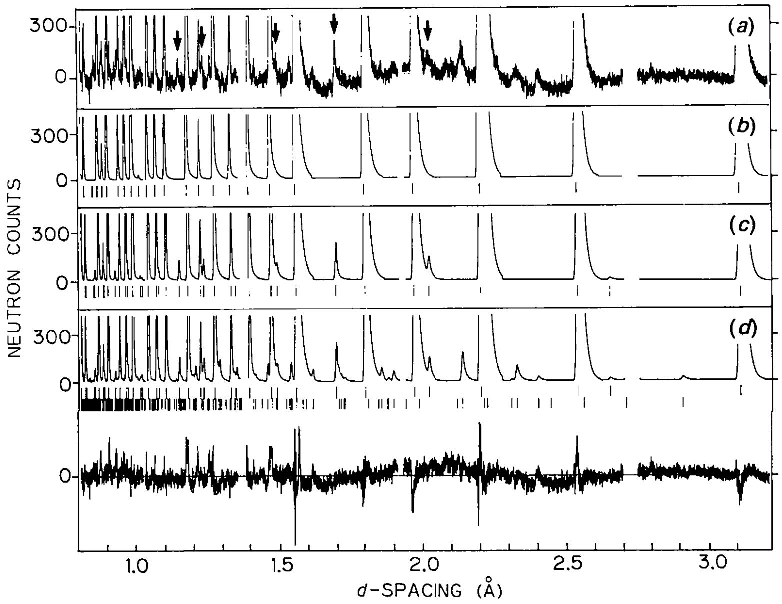

Fig. 1. Observed (*a*) and calculated neutron diffraction profiles for cubic $BaBiO_3$ at 900 K shown on an expanded intensity scale. The background is subtracted from the observed profile. Calculations assume a simple perovskite cell (*b*), a doubled perovskite cell with asymmetric O positions (*c*), and mullite contamination (*d*). The top trace shows a fitted profile, the short vertical bars mark the Bragg peak positions, and the bottom trace in (*d*) shows the intensity differences. Arrows in (*a*) mark superlattice reflections 331, (333, 511), 531, (551, 711) and (553, 731) from right to left. Actual fits include data down to $d = 0{\cdot}5$ Å.

Table 1. *Cell parameters, atomic positions and anisotropic temperature-factor coefficients for* $BaBiO_3$ *and cell parameters for mullite at* 900 K

Equivalent isotropic B factors, B_{eq}, were calculated from β_{ii}'s.

Barium–bismuth oxide $BaBiO_3$
Cubic $Fm\bar{3}m$ (No. 225), $a = 8{\cdot}7676\ (6)$ Å

		x	y	z	β_{11}	β_{22}, β_{33}	B_{eq} (Å^2)
Ba	8(*c*)	0·25	0·25	0·25	0·0075 (2)	0·0075 (2)	2·34 (12)
Bi(1)	4(*a*)	0·0	0·0	0·0	0·0029 (4)	0·0029 (4)	0·99 (21)
Bi(2)	4(*d*)	0·5	0·5	0·5	0·0028 (4)	0·0028 (4)	0·77 (21)
O	24(*i*)	0·2605 (4)	0·0	0·0	0·0038 (4)	0·0205 (3)	4·53 (18)

$R_I = 4{\cdot}19$, $R_F = 6{\cdot}46\%$

Mullite $Al(Al,Si)_2O_{4{\cdot}86}$ (Al:Si = 3:2)
Orthorhombic *Pbam* (No. 55), $a = 7{\cdot}7554\ (2)$, $b = 7{\cdot}7724\ (2)$, $c = 2{\cdot}8973\ (6)$ Å
$R_{wp} = 4{\cdot}22$, $R_p = 3{\cdot}21$, $R_e = 2{\cdot}85\%$

shift of about 0·1 Å away from Bi(1) towards Bi(2). Table 1 lists the final structural parameters; the most noteworthy is the considerable anisotropy in the thermal vibrations of the O ions.

3. Phases and electrical resistivity of oxygen-deficient $BaBiO_{3-x}$

Chaillout, Santoro, Remeika, Cooper, Espinosa & Marezio (1988) claim that the ordering behavior of Bi cations at room temperature depends upon the thermal history of the sample. Materials prepared from the melt show similar average Bi—O distances for the Bi(1) and Bi(2) sites in the monoclinic structure, while those prepared or heat treated at 1073 K exhibit distinct Bi—O distances for the two sites. These authors combine this behavior with anomalies of DTA (differential thermal analysis) curves and argue that the Bi cations have 4+ valence between the melting point and 1074 K, and disproportionate into Bi^{3+} and Bi^{5+} at 1074 K in air. We pointed out earlier that the reported thermal anomalies are associated with the phase change between phases I and II of oxygen-deficient $BaBiO_{3-x}$ (Kusuhara *et al.*, 1989). In the phase diagram obtained from recent thermogravimetric measurements (Beyerlein, Jacobson & Yacullo, 1985; Saito, Maruyama & Yamanaka, 1987), phase I occupies the range $0 < x \leq 0{\cdot}05$ close to full oxidation. In $BaBiO_{3-x}$ in equilibrium with O_2 gas at 1 kPa, the I→II transition occurs at about 1050 K, and phase II is produced when the material is reduced to $x \simeq 0{\cdot}13$ at the same temperature. The latter phase becomes unstable at $x \simeq 0{\cdot}35$, and transforms into phase III at about 1130 K, which exists for $0{\cdot}42 \leq x \leq 0{\cdot}5$. Similar phase relations were also obtained from coulometric measurements (Maruyama, Yamanaka & Saito, 1989). Our *in-situ* X-ray diffraction data reveal that phases I and II are not single phases, but mixtures of two structures showing cubic and tetragonal symmetries. The former is a much more abundant component in both mixtures (Kusuhara *et al.*, 1989).

If the valence state of Bi is represented as $Ba_2Bi^{3+}Bi^{5+}O_{6-2x}$ in phase I and $BaBi^{4+}O_{3-x}$ in phase II as proposed by Chaillout *et al.* (1988), semiconducting and metallic properties would be expected for phase I and II materials, respectively. To confirm this, we have undertaken an electrical resistivity measurement on sintered $BaBiO_{3-x}$ pellets in Ar 99% + O_2 1% gas at atmospheric pressure (oxygen partial pressure 1 kPa). The samples were mounted with gold contacts in a furnace, and a standard four-probe DC method was used with minimal current. Fig. 2 shows typical results. A decreasing resistivity over the range 290–1040 K confirms the semiconductor-like properties of the three oxidized phases of $BaBiO_3$ and phase I of oxygen-deficient $BaBiO_{3-x}$. However, the temperature dependence is describable by a well-defined activation energy only in the monoclinic phase (~0·27 e V). The gradual change at about 1000 K coincides with the onset of conspicuous oxygen deficiency in $BaBiO_{3-x}$. There was some indication of a small discontinuity at 1040 K, where the I→II phase transition occurred. This is followed by a nearly linear increase, which is interrupted by a large upward jump at about 1100 K, owing to the II→III phase transition. The latter process was extremely slow so that a transient resistivity was recorded 12 h after the temperature variation. On cooling the sample, the same resistivity curve was closely traced back with no hysteresis over

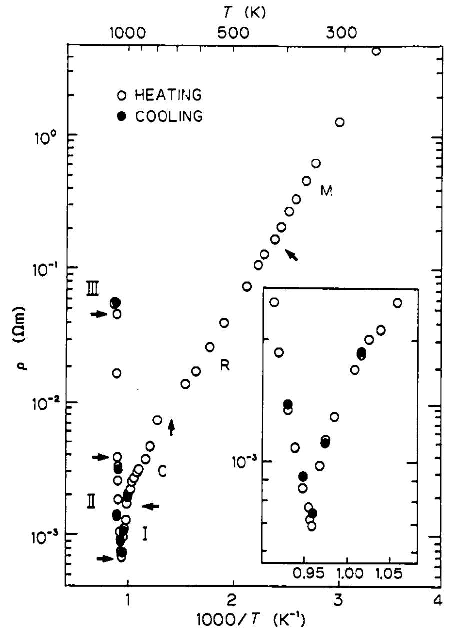

Fig. 2. Electrical resistivities of $BaBiO_{3-x}$ in O_2 gas under 1 kPa partial pressure plotted against inverse temperature. Segments *M*, *R* and *C* correspond to the monoclinic, rhombohedral and cubic phases of fully oxidized $BaBiO_3$, while I, II and III refer to phases I, II and III respectively, of oxygen-deficient $BaBiO_{3-x}$.

the temperature range studied. These observations show quite unambiguously a reversible semiconductor–metal-like transition at the I–II phase boundary.

4. Structures of phase I and phase II compounds

The quite different electrical behavior of phase I and II materials invited us to examine the neutron powder data collected from $BaBiO_{3-x}$ at 1025 and 1075 K in O_2 gas under a partial pressure of 1 kPa. As reported previously, these data show unresolved cubic and tetragonal reflections. Rietveld refinements were conducted on a three-component system with orthorhombic mullite as the third component. For the tetragonal component of $BaBiO_{3-x}$ we assumed a body-centered *I*4/*mmm* cell with edges $a_t \simeq 2^{1/2}a_0$ and $c_t \simeq 2a_0$ instead of the primitive *P*4/*mmm* cell used in the previous analysis.

The 1025 K data were refined for each of the simple and the doubled perovskite-cell models for cubic $BaBiO_{3-x}$. The initial structural parameters were taken from the previous X-ray results, and the O position in the latter model was allowed to vary. Site-occupancy parameters were refined for both cubic and tetragonal $BaBiO_{3-x}$, but the cubic component showed no significant oxygen deficit. The doubled-cell model gave slightly lower *R* values than the simple-cell model with an O position moved to $x(\mathrm{O}) = 0{\cdot}2593\ (5)$ (Table 2). This is virtually identical to the results found in $BaBiO_3$ at 900 K, illustrating a remarkable rigidity of the BiO_6 octahedra and thereby supporting the ordered Bi arrangement in the phase I cubic structure. The actual profile fit is shown in Fig. 3, where the finite-intensity superlattice peaks are satisfactorily fitted. The refined scale factors indicate that the tetragonal component occupies 3% of the diffracting sample weight. The refined site-occupancy parameters, on the other hand, show an oxygen deficit of $x = 0{\cdot}36$ for the tetragonal structure. On combining these results, we find an overall oxygen deficit of $x = 0{\cdot}01$ for $BaBiO_{3-x}$ compounds at 1025 K, which is close to the value of 0·02 estimated from the phase diagram.

Table 2. *Cell parameters, atomic positions, anisotropic temperature-factor coefficients and site-occupancy factors (g) for phase* I *of* $BaBiO_{3-x}$ *at* 1025 K *in* O_2 *gas under* 1 kPa *partial pressure*

Equivalent isotropic *B* factors, B_{eq}, were calculated from β_{ii}'s. The *B*-factor values for the tetragonal component were taken from intermediate cubic results and not refined.

Barium–bismuth oxide $BaBiO_{3-x}$
Cubic $Fm\bar{3}m$ (No. 225), $a = 8{\cdot}7871\ (7)$ Å

		x	y	z	β_{11}	β_{22}, β_{33}	B_{eq} (Å^2)
Ba	8(*c*)	0·25	0·25	0·25	0·0087 (2)	0·0087 (2)	2·78 (7)
Bi(1)	4(*a*)	0·0	0·0	0·0	0·0033 (5)	0·0033 (5)	1·14 (14)
Bi(2)	4(*d*)	0·5	0·5	0·5	0·0032 (4)	0·0032 (4)	0·93 (14)
O	24(*i*)	0·2593 (5)	0·0	0·0	0·0051 (4)	0·0219 (3)	4·96 (9)

$R_I = 4{\cdot}50$, $R_F = 6{\cdot}47\%$

Tetragonal *I*4/*mmm* (No. 139), $a = 6{\cdot}287\ (1)$, $c = 9{\cdot}029\ (2)$ Å

		x	y	z	B (Å^2)	g
Ba	4(*d*)	0·0	0·5	0·25	2·80	1·0
Bi(1)	2(*a*)	0·0	0·0	0·0	1·04	1·0
Bi(2)	2(*b*)	0·0	0·0	0·5	0·96	1·0
O(1)	8(*h*)	0·17 (1)	0·17 (1)	0·0	5·26	0·8 (1)
O(2)	4(*e*)	0·0	0·0	0·28 (1)	5·26	0·96 (15)

$R_I = 37{\cdot}86$, $R_F = 17{\cdot}15\%$

Mullite $Al(Al,Si)_2O_{4{\cdot}86}$ (Al:Si = 3:2)
Orthorhombic *Pbam* (No. 55), $a = 7{\cdot}7558\ (2)$, $b = 7{\cdot}7724\ (2)$,
$c = 2{\cdot}9001\ (6)$ Å
$R_{wp} = 3{\cdot}63$, $R_p = 2{\cdot}97$, $R_e = 2{\cdot}26\%$

The 1075 K data exhibit no obvious superlattice peaks from cubic $BaBiO_{3-x}$ (Fig. 4). The refinement was accordingly based upon a simple perovskite cell for cubic $BaBiO_{3-x}$ and an *I*4/*mmm* cell for the tetragonal component. The oxygen site-occupancy parameters were included in the refinement for both cubic and tetragonal components. Agreement between the observed and calculated profiles was less satisfactory than in the previous cases because of the lower neutron counts in the 1075 K data. However, the quality of the fit ($R_{wp} = 4{\cdot}69$, $R_p = 3{\cdot}61$, $R_e = 3{\cdot}91$, $R_I = 4{\cdot}76$ and $R_F = 7{\cdot}83\%$) apparently supports the simple perovskite structure with one $BaBiO_{3-x}$ formula unit per unit cell for the cubic component of the phase II material. As for the tetragonal component the refined value of *c* is about 1% greater than that at 1025 K, in agreement with the previous X-ray observations. The refined scale factors show a weight fraction of 8% for the tetragonal component, while the site-occupancy parameters indicate oxygen deficits of $x = 0{\cdot}12$ and 1·2 for the cubic and tetragonal components, respectively. These yield an overall deficit of $x = 0{\cdot}3$, which agrees surprisingly well with 0·2 estimated from the phase diagram. One cannot, however, attribute much quantitative significance to this agreement in view of the poor intensity agreement in the weak tetragonal reflections.

5. Discussion and concluding remarks

It seems very likely that the crystallographic position of O ions in cubic $BaBiO_{3-x}$ structures is controlled by oxygen defects. In cubic $BaBiO_3$ containing little or no oxygen defects, nearly all O ions are shifted, which would promote the disproportionation of Bi^{4+} into Bi^{3+} and Bi^{5+} to give an energetically more-favored ordered arrangement. An oxygen vacancy produces a pair of Bi cations facing each other. This unfavorable configuration would lead to the formation of defect complexes involving positional shifts of nearby O ions and charge redistribution. At a certain level of defect concentration, the breathing-mode oxygen displacement in the matrix crystal would be cancelled, and disproportionated Bi cations would be integrated by electron transfer. One can also speculate that the complexes produced would have tetragonal symmetry.

Clearly, the electrical conductivity of nonstoichiometric $BaBiO_{3-x}$ at high temperatures is dominated by the oxygen-defect concentration. Indeed, at a fixed temperature $BaBiO_{3-x}$ shows monotonically increasing resistivities as x increases over the whole range $x = 0$–$0{\cdot}5$ (Yamanaka, 1990). Metallic properties cannot therefore be assigned to phase II materials on the basis of the observed positive temperature coefficient of resistivity. Nevertheless, the reversed temperature coefficients for phase I and II materials are beyond doubt, and should find explanation in the observed structural differences between the two materials.

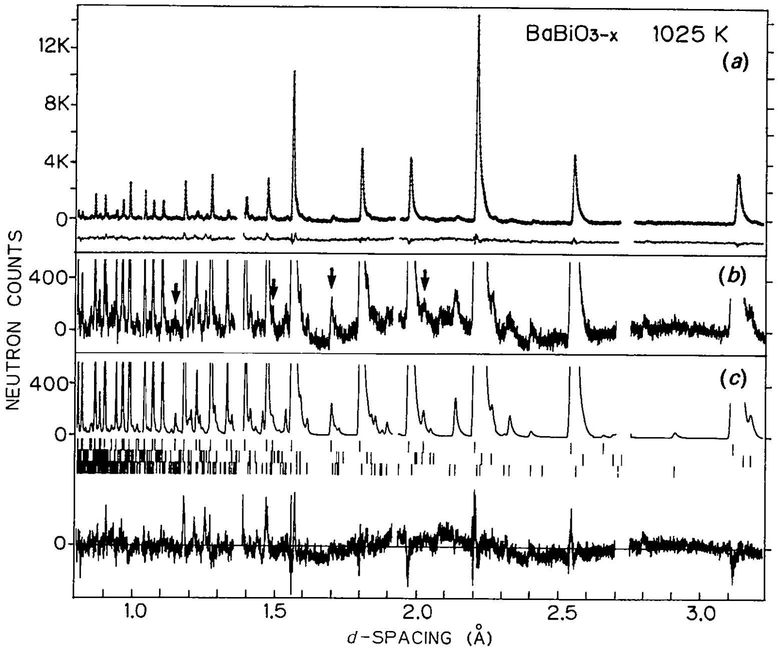

Fig. 3. Observed and calculated powder patterns for $BaBiO_{3-x}$ in phase I. The sample is kept at 1025 K in O_2 gas under 1 kPa partial pressure. In (*a*) crosses denote observed intensities and the line shows calculations with difference plots at the bottom. The profile fit is based upon a doubled perovskite cell with asymmetric O positions for cubic $BaBiO_{3-x}$, a body-centered cell for tetragonal $BaBiO_{3-x}$ and an orthorhombic cell for mullite. (*b*) and (*c*) display observed and calculated profiles, respectively, on an expanded intensity scale. The bottom trace in (*c*) shows the intensity differences. Superlattice peaks are marked by arrows in (*b*).

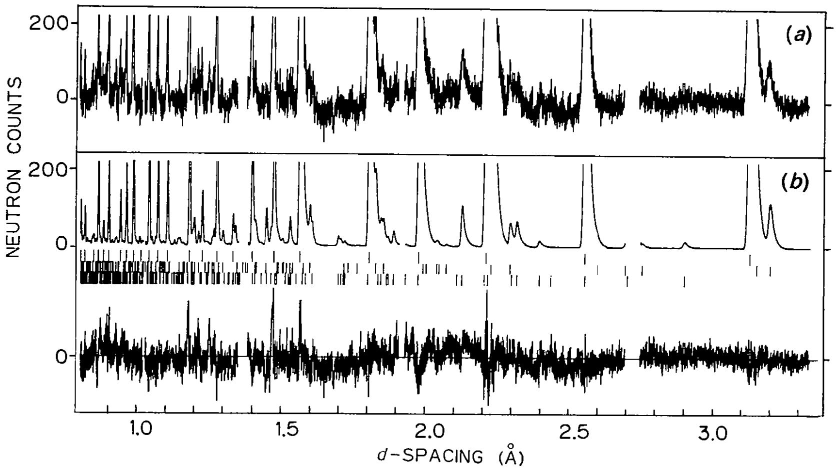

Fig. 4. Observed (*a*) and calculated (*b*) profiles for phase II of $BaBiO_{3-x}$ at 1075 K shown on an expanded scale. The calculation assumes a simple perovskite cell for cubic $BaBiO_{3-x}$, a body-centered cell for tetragonal $BaBiO_{3-x}$ and includes mullite contamination. The intensity differences are shown at the bottom of (*b*).

In conclusion, we have shown that cubic BaBiO$_3$ contains a breathing-mode distortion resulting from the shifted O ions. This can be interpreted in terms of an ordered array of Bi^{3+} and Bi^{5+} cations. The structural features survive in phase I of oxygen-deficient BaBiO$_{3-x}$, where the oxygen deficit is likely to be entirely accounted for by the coexisting tetragonal component. The ordered Bi arrangement in cubic BaBiO$_3$ is consistent with the semiconductor-like properties of the material, which have been shown to extend into phase I. In more-reduced phase II compounds both cubic and tetragonal structures appear to be oxygen deficient. The lack of the breathing-mode distortion in the cubic structure tempts us to favor the 4+ valence state for the Bi cations, which does not contradict the metal-like properties of the phase II material. The real structures of the tetragonal phases are still obscure owing to their low concentrations in the mixtures.

The authors thank F. Izumi for the generous provision of the revised *RIETAN* program. Suggestions from T. Maruyama on the method of resistivity mesurement are appreciated. This work is supported by KENS and The Asahi Glass Foundation.

References

Beyerlein, R. A., Jacobson, A. J. & Yacullo, L. N. (1985). *Mater. Res. Bull.* **20**, 877–886.
Chaillout, C., Santoro, A., Remeika, J. P., Cooper, A. S., Espinosa, G. P. & Marezio, M. (1988). *Solid State Commun.* **65**, 1363–1369.
Cox, D. E. & Sleight, A. W. (1976). *Solid State Commun.* **19**, 969–973.
Cox, D. E. & Sleight, A. W. (1979). *Acta Cryst.* **B35**, 1–10.
Hair, J. de & Blasse, G. (1973). *Solid State Commun.* **12**, 727–729.
Izumi, F., Asano, H., Murata, H. & Watanabe, N. (1987). *J. Appl. Cryst.* **20**, 411–418.
Kusuhara, H., Yamanaka, A., Sakuma, H. & Hashizume, H. (1989). *Jpn. J. Appl. Phys.* **28**, 678–684.
Maruyama, T., Yamanaka, A. & Saito, Y. (1989). *Solid State Ionics*, **36**, 121–126.
Mattheiss, L. F. & Hamann, D. R. (1983) *Phys. Rev. B*, **28**, 4227–4241.
Orchard, A. F. & Thornton, G. (1977). *J. Chem. Soc. Dalton Trans.* pp. 1238–1240.
Rietveld, H. M. (1969). *J. Appl. Cryst.* **2**, 65–71.
Saalfeld, H. & Guse, W. (1981). *Neues Jahrb. Mineral. Monatsh.* pp. 145–150.
Saito, Y., Maruyama, T. & Yamanaka, A. (1987). *Thermochim. Acta*, **115**, 199–205.
Wertheim, G. K., Remeika, J. P. & Buchanan, D. E. (1982). *Phys. Rev. B*, **26**, 2120–2123.
Yamanaka, A. (1990). *Nonstoichiometry and Crystal Structures of Barium-Bismuth Oxides*. PhD Thesis, Tokyo Institute of Technology, Japan.
Young, R. A. & Wiles, D. B. (1982). *J. Appl. Cryst.* **15**, 430–438.

Acta Cryst. (1990). **B46**, 698–702

Structure of a Ferroelectric and Ferroelastic Monodomain Crystal of the Perovskite BiFeO$_3$

By F. Kubel and H. Schmid

*Département de Chimie Minérale, Analytique et Appliquée, Université de Genève, CH-*1211 *Genève* 4, *Switzerland*

(*Received* 25 *September* 1989; *accepted* 15 *June* 1990)

Abstract

X-ray diffraction data on a ferroelectric and ferroelastic monodomain single crystal of BiFeO$_3$ at 294 K are reported. Bismuth iron oxide, M_r = 312·83, $R3c$, λ(Mo $K\alpha$) = 0·7107 Å, $a_{\rm hex}$ = 5·57874 (16), $c_{\rm hex}$ = 13·8688 (3) Å, $V_{\rm hex}$ = 373·802 (17) Å^3, $a_{\rm rh}$ = 5·6343 Å, $\alpha_{\rm rh}$ = 59·348°, $V_{\rm rh}$ = 124·601 Å^3, Z = 6, D_x = 8·337 Mg m^{-3}, μ = 75·97 mm^{-1}, F(000) = 798, R = 2·4, wR = 1·9% for 422 independent reflections. The structure can be described as a rhombohedrally distorted simple cubic perovskite cell. The oxygen octahedron is distorted with minimum and maximum O—O distances of 2·710 (7) and 3·015 (9) Å, respectively, and rotated by about $\pm\alpha$ = 13·8 (3)° around the threefold axis. The iron atom is shifted away from the centre of the deformed oxygen octahedron by about 0·134 (7) Å along the threefold axis. The bismuth atom is shifted with respect to two neighbouring octahedron centres by about 0·540 (7) Å along the threefold axis. Bi—Fe distances are 3·0617 (11) and 3·8726 (11) Å. The oxygen atom is displaced by 0·2877 (6) Å away from the Bi$_4$ plane. The iron–oxygen chain has angles of 165·04 (21) (O—Fe—O) and 154·1 (4)° (Fe—O—Fe), and dihedral angles of 127·8 (9) (O—Fe—O—Fe) and 121·6 (9)° (Fe—O—Fe—O). The ferroelectric poling mechanism was analyzed: atom displacements

0108-7681/90/060698-05$03.00